AIChE

Sorption Dynamics in Fixed-Beds of Inert Core Spherical Adsorbents Including Axial Dispersion and Langmuir Isotherm

M. Khosravi Koocheksarayi and K. Shams
Dept. of Chemical Engineering, Isfahan University of Technology, Isfahan 84156-83111, Iran

Y. Z. Liu
Dept. of Chemical Engineering, Xi'an Jiaotong University, Xi'an, China

DOI 10.1002/aic.11832
Published online June 4, 2009 in Wiley InterScience (www.interscience.wiley.com).

The effects of axial dispersion and Langmuir isotherm on transient behavior of sorption and intraparticle diffusion in fixed-beds packed with monodisperse shell-type/inert core spherical sorbents are studied. The system of partial differential equations of the mathematical model is solved numerically using finite difference methods. Results are presented in the form of breakthrough curves for adsorption and desorption processes. Results reveal that the shape of the breakthrough curves is influenced by both hydrodynamic and kinetic factors. Hydrodynamic factor is governed by axial dispersion and is controlled by changes of Peclet number. Simulation results reveal that when linear adsorption isotherm is used, the effect of axial dispersion on breakthrough curves of the system is important for Peclet numbers smaller than 50, whereas, for Langmuir isotherm axial dispersion is considerable for Peclet numbers less than 80. In addition, effects of type of adsorption isotherms and size of adsorbents on breakthrough curves are investigated, and results are compared with existing reports in the pertinent literature. © 2009 American Institute of Chemical Engineers *AIChE J,* 55: 1784–1792, 2009
Keywords: inert core adsorbent, fixed-bed, shell-type adsorbent, sorption, Langmuir isotherm, breakthrough curve, mass transfer, adsorption

Introduction

Separation maybe defined as a process that transforms a mixture of substances into two or more products that differ from each other in composition. The separation steps often account for the major production costs in chemical and petrochemical industries. Adsorption and desorption are widely used as separation operations in process industries, chromatographic techniques, ion exchange between solutions and solids, catalytic reactions, drying, distillation, enzyme and protein purification, power generation, and food industries.

Correspondence concerning this article should be addressed to K. Shams at k_shams@cc.iut.ac.ir

The fixed-beds that are utilized for adsorption and desorption operations are characterized by a concentration wave front the shape of which indicates the degree of separation that can be achieved. The concentration wave front in adsorbers/desorbers is conveniently demonstrated through standard diagrams that are commonly called breakthrough curves, and have significant value in terms of design, operation, and control of these systems. It has been established that breakthrough curves are influenced by both hydrodynamic (i.e., axial dispersion) and kinetic (i.e., finite transport rates) factors. Nature and type of adsorption isotherms, size distribution and geometry of packing particles, and system geometry are other factors that affect the shape of breakthrough curves. Using monodisperse spherical particles/beads as sorbent in sorption columns is a matter of common

practice, and there is a large body of theoretical and experimental literature available on various aspects of fixed beds packed with solid spherical sorbents.[1–26]

Extensive review of the existing literature in the realm of adsorption/desorption processes in packed beds reveals that most of the studies are limited to the analysis of fixed beds of solid spherical particles. Furthermore, in all the existing monodisperse spherical models, linear sorption isotherm and intraparticle diffusion are considered and zero flux boundary condition at the center of the spherical particles due to the symmetry is applied. To a certain extent, this combination of linear isotherm and simple symmetry boundary condition makes analytic and numerical solutions to the system of describing equations simple. However, there are situations with significant practical implications where this condition does not hold. For instance, in dielectric coating processes, controlled release from encapsulated drugs, grain drying, and olive pickling in food industries are situations where one encounters with mass transfer in a configuration, which essentially may be considered as a spherical solid shell/hollow sphere, or a sphere with an inert core. The number of published articles on the treatment of problems associated with beds of inert core adsorbents/shell-type geometries is highly limited. Shams[27] modeled the transient behavior of adsorption/desorption from a fixed-bed packed with thin-film-coated spherical particles/hollow spheres where axial dispersion and external mass-transfer resistance are negligible. He solved mass transfer equations analytically and could get breakthrough curves for system parameters through numerical integration of an infinite integral. Li et al.[28] modeled breakthrough and elution curves in a fixed-bed of inert core adsorbents. They derived new analytical solutions to predict breakthrough and elution curves for linear adsorption systems coupled with axial dispersion, film mass transfer, and intraparticle mass transfer. Furthermore, in the last decade, inert core adsorbents have been used to improve the separation performance of proteins in expanded-bed adsorbers.[29–33] Large-pore supports in chromatographic processes have been used to reduce the mass transfer resistance.[34] Nonporous beads have been suggested to overcome film mass transfer resistance in fixed beds.[35] Particles with a thin layer of porous silica on a solid inert core have been practiced to improve the sorption efficiency in high-performance resolution of protein in liquid-chromatography.[36,37] Also, in the manufacture of shell-type catalysts for catalytic converters in auto industries, the active ingredients are deposited in the form of a skin or shell on the outside portion of an inert core or substrate.[38] In all of these situations, previous results related to spherical sorbents cannot fully predict the sorption behavior of the bed.

The objective of this work is to derive sorption breakthrough curves in a fixed-bed system consisting of monodisperse inert core/shell-type/hollow spherical sorbents, where axial dispersion plays an active role and the Langmuir adsorption isotherm describes the equilibrium exchange between the moving and stationary phases. Nonlinear exchange law makes the problem nonlinear. Therefore, the descriptive system equations are amenable to solution by numerical methods. In the ensuing sections, the problem statement is explained, governing equations are developed, system equations are solved numerically, and the results are discussed.

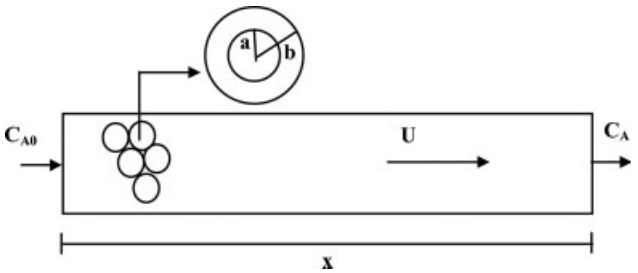

Figure 1. Fixed-bed packed with inert core/shell-type/hollow spherical sorbent particles.

Problem Statement

Consider a bed packed with monodisperse inert core/shell-type/hollow spherical sorbent particles. The spherical particles are uniformly distributed throughout the bed with a void fraction of ε and contain a desorbable component A in the shell, or A may diffuse through the shell from the flowing phase. The thickness of the film/shell is equal to $(b-a)$, where a and b are the inner and the outer radii of the spherical particles, respectively, as shown in Figure 1. A fluid flows through the bed at the entrance with a constant linear superficial velocity U. The goal is to obtain the dynamic response of sorption of the bed when subjected to a step change in feed concentration at time zero.

Theoretical Development and System Modeling in the Sorption Process

Following Rosen[5] and Shams[27] we make the following simplifying assumptions:

1. The system is at uniform temperature.
2. Sorbent particles are small compared with the diameter and length of the bed.
3. The external mass transfer resistance is negligible.
4. We may describe the intraparticle diffusion of A within the shell by Fick's law of diffusion.
5. Axial dispersion is considered.

Furthermore, desorption equilibrium of the desorbable component A follows a nonlinear Langmuir-type isotherm. In light of the above assumptions, the spatiotemporal behavior of the concentration of the sorbed component in the effluent stream can be computed from equations derived from performing mass balances on mobile and stationary phases presented in the next section.

Mobile Phase Mass Balances

An unsteady-state shell mass balance on mobile phase gives:

$$\frac{\partial C_A}{\partial t} = -U\frac{\partial C_A}{\partial x} + D\frac{\partial^2 C_A}{\partial x^2} \pm \frac{3(1-\varepsilon)D_A}{\varepsilon b}\frac{\partial q}{\partial r}\Big|_{r=b} \quad (1)$$

$$\text{at } x = 0 : C_A = 0 \quad (2)$$

$$\text{at } x = L : \frac{\partial C_A}{\partial x} = 0 \tag{3}$$

$$\text{at } t = 0, \text{ yet to be defined}$$

where C_A is the concentration of A in the mobile phase, D is the axial dispersion coefficient, D_A is the intraparticle diffusion coefficient, x is the axial coordinate of the bed, ε is the void fraction of the bed, r is the radius of sorbent particles, and L is the length of the bed. Furthermore, in Eq. 1 the plus sign in front of the last term stands for adsorption, whereas the minus sign indicates desorption. The second boundary condition given above (i.e., Eq. 3) is the famous Neumann or second type boundary condition, which is mostly used in packed beds. For getting the initial condition needed, we assume that at time zero equilibrium condition throughout the bed is established and from the nonlinear Langmuir isotherm, this initial condition will be determined and explained when the model equations are made dimensionless.

Stationary Phase Mass Balances

A transient shell mass balance on the stationary phase gives:

$$\frac{\partial q}{\partial t} = \frac{D_1}{r^2}\frac{\partial}{\partial r}\left(r^2\frac{\partial q}{\partial r}\right) \tag{4}$$

One can recast this equation as:

$$\frac{\partial^2}{\partial r^2}(rq) - \frac{1}{D_1}\left(\frac{\partial}{\partial t}(rq)\right) = 0 \tag{5}$$

Subject to:

$$\text{at } t = 0 : \; q(x, 0, r) = q_o \tag{6}$$

$$\text{at } r = a : \; \frac{\partial q}{\partial r} = 0 \quad \forall t \tag{7}$$

at $r = b$, this boundary condition depends on equilibrium exchange law and will be given and discussed in the next section.

Nondimensionalization of Model Equations

The system equations are made dimensionless using the following dimensionless variables:

$$\text{Dimensionless length: } \zeta = \frac{x}{L} \tag{8}$$

$$\text{Dimensionless time: } \tau = \frac{Ut}{L} \tag{9}$$

$$\text{Dimensionless radius of solid particles: } \rho = \frac{r}{b-a} \tag{10}$$

To define initial conditions in mobile and stationary phases and boundary condition at the edge of the solid pellets, and prescribe dimensionless concentrations for both phases, Langmuir isotherm must be considered. Langmuir equilibrium relation is given as

$$\frac{q}{q_s} = \frac{BC_A}{1 + BC_A} \tag{11}$$

where, q is the concentration of A in solid phase, q_s is the saturated concentration of the solid phase, C_A is the concentration of A in the mobile phase, and B is a constant. For a suitable description of dimensionless concentration of solid phase, we assume at time zero solid phase is saturated by % 90. Therefore, $q_0 = 0.9q_s$. The reason that at the time zero the bed is not considered to be fully saturated is imbedded in Langmuir isotherm. Generally, the Langmuir isotherm implies that when concentration in solid phase approaches the saturated concentration, q_s, the mobile phase concentration approaches infinity; this is readily verified by rephrasing the Langmuir isotherm as follows:

$$C_A = \frac{\frac{q}{q_s}}{B\left(1 - \frac{q}{q_s}\right)} \tag{12}$$

Further, to complete the nondimensionalization process, the following dimensionless variables are introduced:

$$\text{Dimensionless concentration in mobile phase: } \theta = \frac{BC_A}{9} \tag{13}$$

Dimensionless concentration in stationary phase:

$$\phi = \frac{q}{q_s} = \frac{0.9q}{q_0} \tag{14}$$

Using the introduced dimensionless concentrations, Eq. 12 becomes

$$\theta = \frac{\phi}{9(1-\phi)} \tag{15}$$

Thus, the initial conditions necessary for the mobile and solid phases are as follows:

$$\text{at } \tau = 0, \theta = 1, \text{ mobile phase} \tag{16}$$

$$\text{at } \tau = 0, \phi = 0.9, \text{ stationary phase} \tag{17}$$

It follows that the system equations and the pertinent boundary and initial conditions in dimensionless form become:

Mobile phase

$$\frac{\partial\theta}{\partial(\sigma\tau)} = -\frac{\gamma'}{\sigma}\frac{\partial\theta}{\partial(\gamma'\zeta)} + \frac{(\gamma')^2}{\sigma}\frac{1}{Pe}\frac{\partial^2\theta}{\partial(\gamma'\zeta)^2} \pm \frac{\gamma'}{\sigma}\frac{b}{(b-a)}\frac{\partial\phi}{\partial\rho}\Big|_{\rho=\frac{b}{(b-a)}} \tag{18}$$

$$\text{at } \zeta = 0 : \theta = 0 \tag{19}$$

$$\text{at } \zeta = 1 : \frac{\partial\theta}{\partial(\gamma'\zeta)} = 0 \tag{20}$$

$$\text{at } \tau = 0 : \theta = \frac{\phi}{9(1-\phi)} \xrightarrow{\tau = 0:\ \phi = 0.9} \theta = 1 \tag{21}$$

Stationary phase

$$\frac{1}{\rho}\frac{\partial \phi}{\partial \rho}+\frac{1}{2}\frac{\partial^2 \phi}{\partial \rho^2}-\frac{\partial \phi}{\partial(\sigma\tau)}=0 \tag{22}$$

$$\rho=\frac{a}{b-a}:\frac{\partial \phi}{\partial \rho}=0 \tag{23}$$

$$\rho=\frac{b}{b-a}:\theta=\frac{\phi}{9(1-\phi)} \tag{24}$$

$$\text{at } \tau=0 \ : \phi=0.9 \tag{25}$$

where, $Pe=\frac{UL}{D}$ is the Peclet number, and the dimensionless parameters γ' and σ are reciprocals of two modified Peclet numbers that indicate the relative importance of Fickian (molecular) diffusion and convection in the mobile and stationary phases, respectively. These dimensionless groups are defined as follows:

$$\gamma'=\frac{3(1-\varepsilon)D_{\mathrm{A}}LBq_{\mathrm{s}}}{9\varepsilon b^2U} \tag{26}$$

$$\sigma=\frac{2LD_{\mathrm{l}}}{(b-a)^2U} \tag{27}$$

Numerical Solution of Dimensionless Mass Balance Equations

Dimensionless mass balance equations in the mobile and stationary phases are a set of coupled nonlinear partial differential equations, and amenable to numerical solution using finite difference methods.

The independent variables of the system equations are $\gamma'\zeta$, ρ, and $\sigma\tau$, and their steps sizes are defined $\Delta(\gamma'\zeta)$, $\Delta\rho$, and $\Delta(\sigma\tau)$, respectively. The discretization of the model equations and the computational procedure is briefly presented in the Appendix.

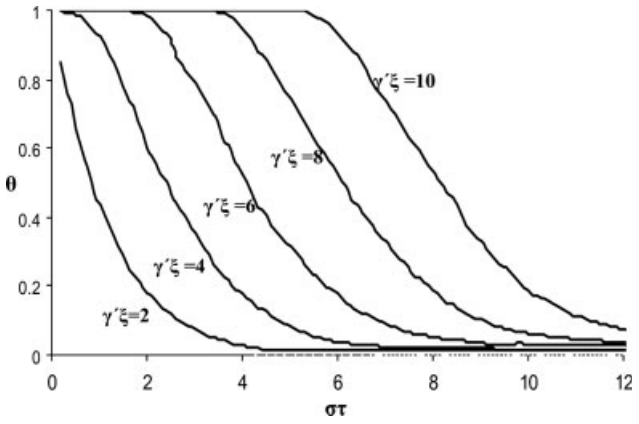

Figure 2. Breakthrough curves in desorption process with axial dispersion and nonlinear isotherm (*Pe* = 10).

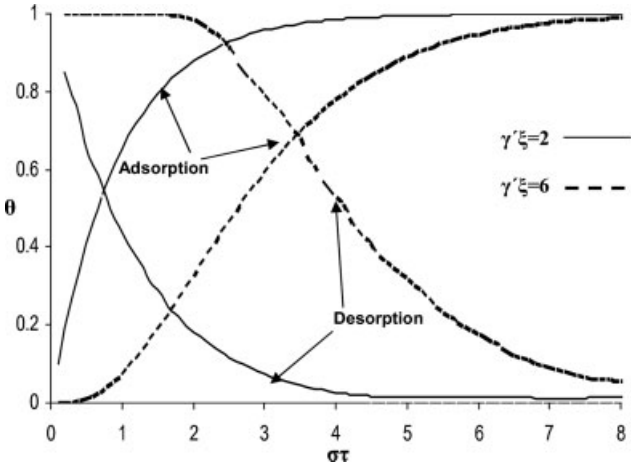

Figure 3. Breakthrough curves in adsorption and desorption processes with axial dispersion and nonlinear isotherm (*Pe* = 10).

Numerical Results and Discussion

Breakthrough curves

Figure 2 shows the breakthrough curves for desorption in the general case, where $Pe = 10$, and Langmuir equilibrium isotherm and longitudinal dispersion are both incorporated in the model equations. In Figure 3, the breakthrough curves for both adsorption and desorption processes are shown for the same value of Peclet number. Figures 2 and 3 present the typical behavior of time course of concentration that one expects in adsorption and desorption processes. If axial dispersion is neglected and a linear equilibrium exchange law is used rather than the well-known Langmuir isotherm, then the model equations are degenerated to those reported by Shams.[27] In this situation, as Figure 4 shows, numerical results are in good agreement with the results obtained by the exact solution of the model equations. The deviations demonstrated in this figure are largely attributed to the convergence criteria used in this work and those used by Shams[27] for the

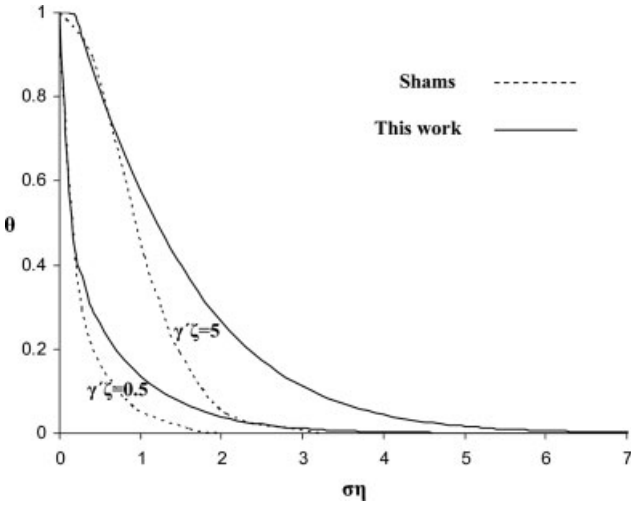

Figure 4. Comparison of results of this work with exact solution[27] at $\gamma'\zeta = 0.5$ and $\gamma'\zeta = 5$.

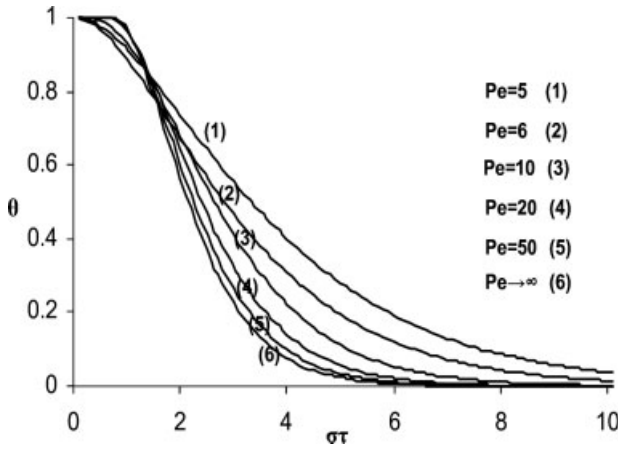

Figure 5. Breakthrough curves in desorption process along with axial dispersion and linear isotherm at $\gamma'\zeta = 6$.

evaluation of an infinite integral, which is the closed form of the exact solution reported by him. This comparison essentially validates the results of the simulations.

Effect of model parameters and exchange law on breakthrough curves

Figures 5 and 6 show effect of the hydrodynamic factor (i.e., axial dispersion) on breakthrough curves; in these curves $Pe \rightarrow \infty$ indicates the condition in which no axial dispersion is present.

It is established that the mass transfer flux along the bed is influenced by convection and axial dispersion. Here, Peclet number is in fact the ratio of mass transfer by convection to mass transfer by dispersion. These results indicate that as Peclet number is increased, the share of mass transfer in the bed by dispersion decreases, and above a certain value of Peclet number the effect of the hydrodynamic factor fades away. Figure 5 shows that when the equilibrium exchange

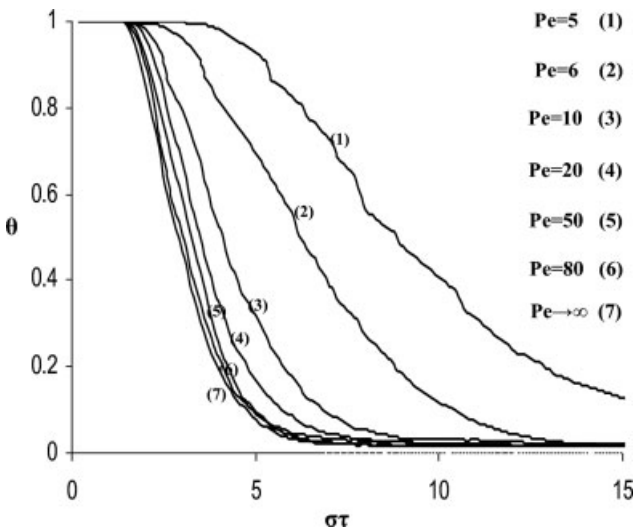

Figure 6. Breakthrough curves in desorption process along with axial dispersion and nonlinear isotherm at $\gamma'\zeta = 6$.

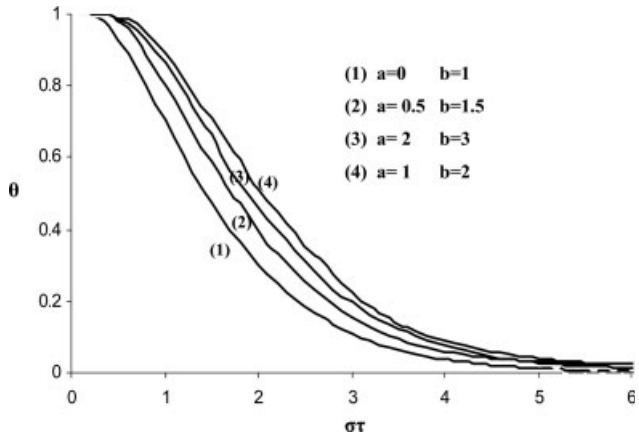

Figure 7. Comparison between full spherical pellets and inert core particles ($Pe = 20$, $\gamma'\zeta = 4$).

law follows a linear function, then axial dispersion plays a role and affects the breakthrough curves only for Peclet numbers of order 50 or less, whereas, this upper limit when nonlinear isotherm is used (see Figure 6), becomes 80. This indicates that when the linear isotherm (e.g., Henry's law) describes the equilibrium exchange, then the hydrodynamic effects become more profound in desorption process.

Figure 7 presents the results obtained to explore the effect of particle size on breakthrough curves. This figure shows that as the particle size becomes larger, it takes a longer time to desorb A out of the shell. This is because the content of A within the shell is larger for larger particles, and the diffusion path is longer. This figure also presents the situation where the inner core radius goes to zero. This situation corresponds to the situation where the bed is packed with monodisperse solid spherical beads.

Figure 8 shows the effects of γ' and σ on breakthrough curves in desorption process along with axial dispersion with

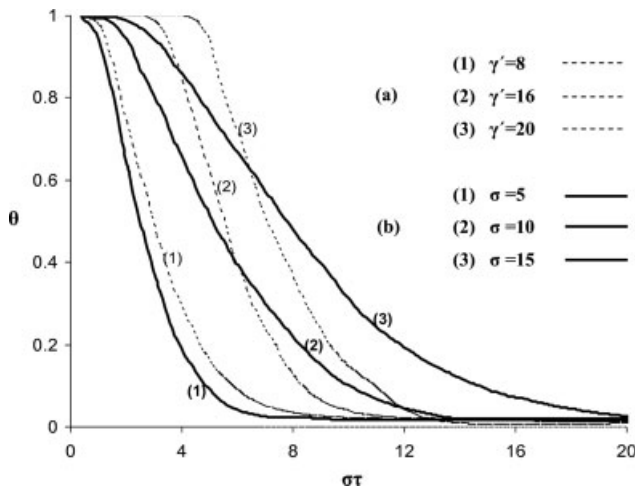

Figure 8. (a) Effect of γ' on breakthrough curves in desorption process along with axial dispersion and nonlinear isotherm ($Pe = 10$, $\zeta = 0.5$); (b) Effect of σ on breakthrough curves in desorption process along with axial dispersion and nonlinear isotherm ($Pe = 10$, $\zeta = 0.4$).

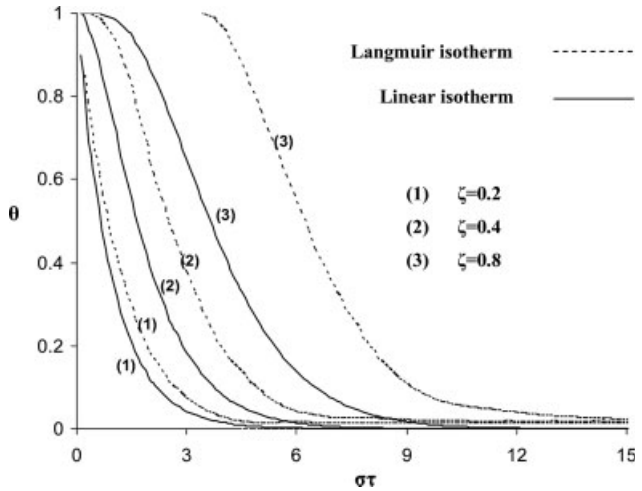

Figure 9. Effect of equilibrium isotherm (linear and nonlinear) on breakthrough curves (*Pe* = 10 at ζ = 0.2, 0.4, and 0.8).

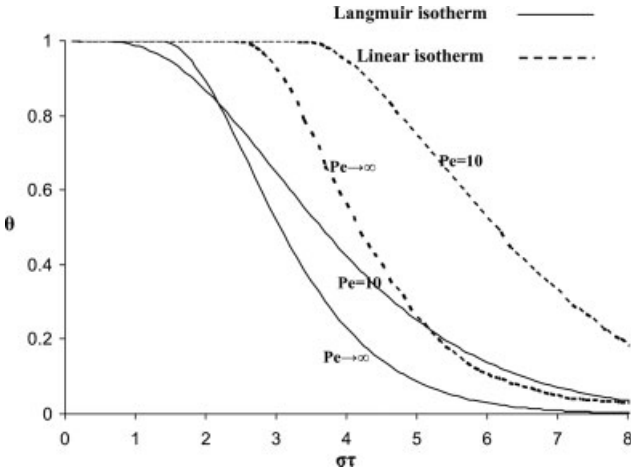

Figure 10. Effect of *Pe* on breakthrough curves using linear and nonlinear isotherms at ζ = 0.8.

nonlinear isotherm, for $Pe = 10$, and $\zeta = 0.5$ and 0.4, respectively.

As mentioned earlier, these two parameters (γ' and σ) are reciprocals of two modified Peclet numbers in the mobile and stationary phases, respectively, that demonstrate the relative significance of molecular diffusion in these two phases, respectively. If linear exchange law is used, these two parameters are modified accordingly as shown in Eqs. 28 and 29.

$$\gamma' = \frac{3(1-\varepsilon)D_A L}{\varepsilon b^2 UH} \tag{28}$$

$$\sigma = \frac{2LD_l}{(b-a)^2 U} \tag{29}$$

These results show that the larger values of γ' and σ translate into less mass transfer by convection, enhanced molecular diffusion in both phases, and subsequently hindrance of desorption process due to the fact that mass transfer is controlled by molecular diffusion, which is inherently a slow process. This adverse effect is more profound when nonlinear isotherm is used.

Figure 9 compares the breakthrough curves of the bed when Langmuir and Henry isotherms are considered as the equilibrium exchange laws at the solid-fluid interface. These results reveal that under the same set of conditions for a given bed, at any given point in time, the concentration of the desorbable component, A, in the mobile phase is larger when Langmuir isotherm is used. Furthermore, the differences between behaviors of the two isotherms become more profound as one gets away from the entrance of the bed. For instance, at $\zeta = 0.2$ the differences between the two isotherms are not appreciable that much, however, as the bed length is increased, ($\zeta = 0.4$, 0.8), the differences of the breakthrough curves for the two isotherms become more profound. Therefore, one concludes that the behavior of the bed does not strongly depend on the type of equilibrium isotherm in the beginning of the bed and for small distances from the entrance, and effect of the nonlinearity of the exchange law becomes important only away from the inlet in the middle and in the end of the bed.

Figures 10 and 11 show the hydrodynamic effects on the breakthrough curves when linear and nonlinear exchange laws are considered. The hydrodynamic effects are compared for $Pe = 10$ and $Pe \to \infty$. These figures show that the hydrodynamic effects are more significant when linear isotherm determines the equilibrium exchange law of the bed. Quantitatively, at dimensionless length of $\zeta = 0.4$, for Langmuir isotherm, when Peclet number is increased from 10 to ∞, the maximum difference of dimensionless concentration of the desorbable component in the mobile phase, θ, is about 0.12, and this quantity almost doubles for linear isotherm. Also, at $\zeta = 0.8$, the maximum reduction of θ in Langmuir isotherm is 0.163 and this increases to 0.502 for the linear isotherm. Therefore, longitudinal dispersion in desorption beds with linear equilibrium exchange law hinders desorption process more effectively than beds that obey Langmuir isotherm.

Comparison of the results with others works

As mentioned earlier, in Figure 4 breakthrough curves obtained from numerical solution of desorption process in

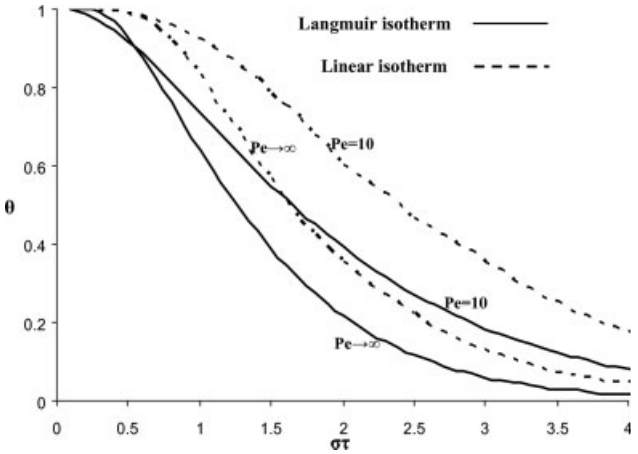

Figure 11. Effect of *Pe* on breakthrough curves using linear and nonlinear isotherms at ζ = 0.4.

fixed-beds packed with inert core spherical particles without axial dispersion and with linear isotherm are compared with exact solution reported by Shams[27] under the same conditions. This comparison is made in Figure 4 at $\gamma'\zeta = 0.5$ and at $\gamma'\zeta = 5$. Results are comparable fairly well with an average difference of about 15% at $\gamma'\zeta = 0.5$ and about 30% at $\gamma'\zeta = 5$, and the discrepancies are mainly because of the convergence criteria used in this work and those used by Shams[27] for evaluation of the infinite integral of the closed form solution.

In Figure 12, the breakthrough curve obtained in this work for adsorption process with axial dispersion and linear isotherm in a fixed-bed packed with monodisperse spherical particles (i.e., when $a = 0$) are compared with the results reported by Raghavan and Ruthven,[10] the results published by Rasmuson and Neretnieks,[8] Rasmuson,[9] and Rosen.[6] The comparison with the results of Rasmuson and Neretnieks[8] and those of Raghavan and Ruthven[10] has been made for $Pe = 19.3$ at $\gamma'\zeta = 2$. One can see that the results are comparable quite well. The average differences between the results obtained in this work are about 10% with respect to those reported by Raghavan and Ruthven and about 8% with respect to the results of Rasmuson and Neretnieks.[8]

The comparison with the results of Rasmuson[9] and Rosen[6] are made at $\gamma'\zeta = 5$. The differences that are observed in comparing these results and the present work are essentially because of different simplifying assumptions that have been made in these works. Rasmuson[9] and Rosen[6] included the external mass transfer resistance in their diffusion models, while it has been intentionally neglected in this work.

Figure 13 shows our results and the results obtained based on an exact solution reported by Li et al.[28] for fixed-beds packed with inert core spherical particles when $a/b = 0.8$. In this figure, we have tried to compare our computational results when axial dispersion and linear exchange law are used with the results reported by this group. One can see that the results are in good agreement, and the differences are because in this work the film resistance has been neglected.

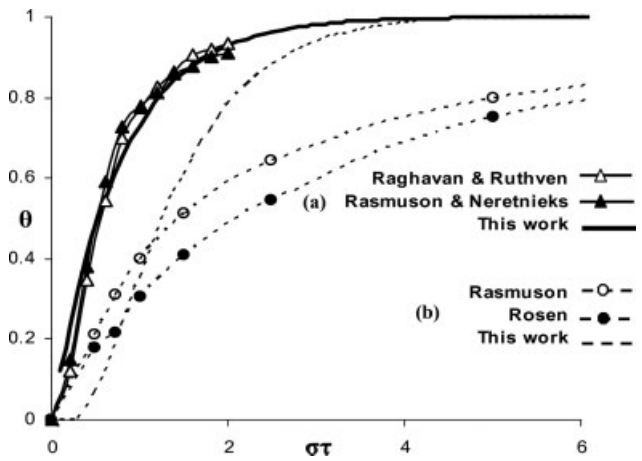

Figure 12. (a) Comparison of breakthrough curves in adsorption process along with axial dispersion from this work and breakthrough curve reported by Rasmuson and Neretnieks,[8] and Raghavan and Ruthven[10]; (b) Comparison of breakthrough curves in adsorption process in the absence of axial dispersion with breakthrough curves published by Rosen[6] and Rasmuson.[11]

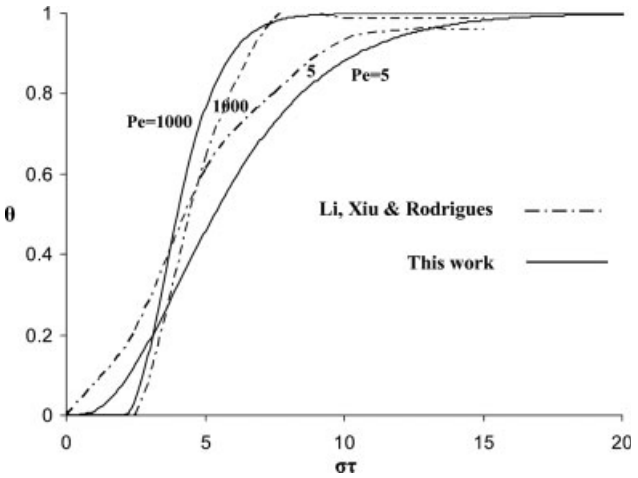

Figure 13. Comparison of breakthrough curves of this work and those reported by Li et al.[28]

Conclusion

The transient behavior of sorption from a fixed-bed packed with monodisperse shell-type/inert core spherical sorbents is studied through mathematical modeling and numerical simulations. Axial dispersion and nonlinear Langmuir equilibrium exchange law are considered. The partial differential equations are solved numerically using finite difference method. The results are presented in the form of breakthrough curves for both desorption and adsorption processes. By changing the values of the system parameters, the results for cases where isotherms are linear and follow Henry's law, longitudinal dispersion is negligible, and monodisperse spherical beads are used as packing could be reproduced. Effects of model parameters are investigated and results are compared with similar works reported in the literature. The results are in good agreement with the existing results and theories. Furthermore, the results show that when linear exchange law is used axial dispersion that represents the hydrodynamic effects plays a role and affects the breakthrough curves only when Pe is less than 50, whereas, when nonlinear isotherm is used hydrodynamic effects become important when Pe is less than 80.

Notation

a = inner radius of spherical particle, m
A' = $(1/(1 - \phi_{i,f,n+1}))$, dimensionless
AA_1 = defined auxiliary function
AA_2 = defined auxiliary function
AA_3 = defined auxiliary function
AA_4 = defined auxiliary function
A_j = defined auxiliary function
b = outer radius of spherical particle, m
B = Langmuir isotherm constant, m^3/kgmol

B_j = defined auxiliary function
C_A = concentration of A in mobile phase, kgmol/m^3
D = axial dispersion coefficient, m^2/s
D_A = diffusivity of A in gas phase, m^2/s
D_j = defined auxiliary function
D_l = diffusivity of A in stationary phase, m^2/s
$E = (-2 + (4\Delta\rho^2/\Delta(\sigma t)))$, dimensionless
$F = (-2 - (4\Delta\rho^2/\Delta(\sigma t)))$, dimensionless
H = linear isotherm constant, dimensionless
K_i = defined auxiliary function
L = bed length, m
Pe = (UL/D) Peclet number, dimensionless
q = concentration of A in coated film/spherical shell, kgmol/m^3
q_0 = initial concentration of A in stationary phase, kgmol/m^3
q_s = saturated concentration of stationary phase, kgmol/m^3
r = radius of spherical particles, m
t = time, s
U = superficial velocity of mobile phase, m/s
x = distance along the x-direction, m

Greek letters

$\gamma' = (3(1 - \varepsilon)D_A LBq_s/9\varepsilon b^2 U)$, dimensionless
ε = bed void fraction, dimensionless
ζ = dimensionless x length of bed in x-direction
$\Delta(\gamma'\zeta)$ = dimensionless distance between two discretization points in x-direction
$\eta = (\tau - \zeta)$, dimensionless
θ = dimensionless concentration of A in flowing phase
ρ = dimensionless radius of spherical particles
$\Delta\rho$ = dimensionless distance between two discretization points in r-direction
$\sigma = (2LD_l/(b - a)^2 U)$, reciprocal of modified Peclet number in sorbent
t = dimensionless time
$\Delta(\sigma t)$ = dimensionless distance between two discretization points in t-direction
φ = dimensionless concentration of A in stationary phase

Subscripts

f = index to specify grid node in r-direction at $r = b$
ff = index to specify grid node in x-direction at $x = L$
i = index to specify grid nodes in x-direction
j = index to specify grid nodes in r-direction
n = index to specify grid nodes in t-dimension

Literature Cited

1. Hougen OA, Marshal WR Jr. Adsorption from a fluid stream flowing through a stationary granular bed. *Chem Eng Prog Trans Sect.* 1947;3:197–208.
2. Thomas HC. Chromatography: a problem in kinetics. *Ann NY Acad Sci.* 1948;49:161–182.
3. Thomas HC. Solid diffusion in chromatography. *J Chem Phys* 1951;19:1213–1233.
4. Rosen JB, Winsche WE. The admittance concept in the kinetics of chromatography. *J Chem Phys.* 1950;18:1587–1592.
5. Rosen JB. Kinetics of a fixed-bed system for solid diffusion into spherical particles. *J Chem Phys.* 1952;20:387–394.
6. Rosen JB. General numerical solution for solid diffusion in fixed-beds. *Ind Eng Chem.* 1954;46:1590–1594.
7. Babcock RE, Green DW, Perry RH. Longitudinal dispersion mechanisms in packed beds. *AIChE J.* 1966;12:922–926.
8. Rasmuson A, Neretnieks I. Exact solution of a model for diffusion in particles and longitudinal dispersion in packed beds. *AIChE J.* 1980;26:686–690.
9. Rasmuson A. Exact solution of a model for diffusion and transient adsorption in particles and longitudinal dispersion in packed beds. *AIChE J.* 1981;27:1032–1035.
10. Raghavan NS, Ruthven DM. Numerical simulation of a fixed-bed adsorption column by the method of orthogonal collocation. *AIChE J.* 1983;29:922–925.
11. Rasmuson A. Exact solution of a model for diffusion in particles and longitudinal dispersion in packed beds: numerical evaluation. *AIChE J.* 1985;31:518–519.
12. Costa C, Rodrigues A. Design of cyclic fixed-bed adsorption processes. *AIChE J.* 1985;31:1645–1654.
13. Cen PL, Yang RT. Analytic solution for adsorber breakthrough curves with bidisperse sorbents (zeolites). *AIChE J.* 1986;32:1635–1641.
14. Raghavan NS, Ruthven DM, Hassan MM. Numerical simulation of a PSA system using a pore diffusion model. *Chem Eng Sci.* 1986;41:2787–2790.
15. Brian BF, Zwiebel I. Numerical simulation of fixed-bed adsorption dynamics by the method of lines. *AIChE Symp Ser.* 1987;83:80–86.
16. Sun LM, Le Quere P, Levan MD. Numerical simulation of diffusion-limited PSA process models by finite difference methods. *Chem Eng Sci.* 1996;51:5341–5352.
17. Xiu GH. Modeling breakthrough curves in a fixed-bed of activated carbon fiber—exact solution and parabolic approximation. *Chem Eng Sci.* 1996;51:4039–4041.
18. Xiu GH, Nitta T, Li P, Jin G. Breakthrough curves for fixed-bed adsorbers: quasi-lognormal distribution approximation. *AIChE J.* 1997;43:979–985.
19. Rodriguez-Maroto JM, Comez-Lahoz C, Vereda-Alonso C, Garcia-Herruzo F, Garcia-Delgado RA. Experimental setup for the study of soil vapor extraction: a practical approach to determine sorption effect. *Water Sci Technol.* 1998;37:169–176.
20. Shams K. Exact solution of a model for in situ volatilization to remediate vadose zone soils. *Iranian J Sci Technol Trans B.* 1999;23:229–238.
21. Coutelieris FA, Kainourgiakis ME, Stubos AK. Low Peclet mass transport in assemblages of spherical particles for two different adsorption mechanisms. *J Colloid Interface Sci.* 2003;264:20–29.
22. Bujan-Nunez MC, Lopez-Quintela MA. Diffusion of a Brownian walker in a bidimensional disordered medium constituted by adsorbing spheres suspended in a solvent. *Mol Phys.* 2004;103:1221–1229.
23. Chang D, Min J, Moon K, Park YK, Jeon JK, Ihm SK. Robust numerical simulation of pressure swing adsorption process with strong adsorbate CO_2. *Chem Eng Sci.* 2004;59:2715–2725.
24. Yamada K, Shibuya M, Takagi C, Hirata M. Adsorption and desorption properties of cationic polyethylene film gels to organic anions and their regeneration. *J Appl Polym Sci.* 2005;99:381–391.
25. Coutelieris FA, Kainourgiakis ME, Stubos AK. Low to moderate Peclet mass transport in assemblages of spherical particles for a realistic adsorption-reaction-desorption mechanism. *Powder Technol.* 2005;159:173–179.
26. Coutelieris FA, Kanavouras A. Experimental and theoretical investigation of packaged olive oil: development of quality indicator based on mathematical predictions. *J Food Eng.* 2005;73:85–92.
27. Shams K. Sorption dynamics of a fixed-bed system of thin-film-coated monodisperse spherical particles/hollow spheres. *Chem Eng Sci.* 2001;56:5383–5390.
28. Li P, Xiu GH, Rodrigues AE. Modeling breakthrough and elution curves in fixed-bed of inert core adsorbents: analytical and approximate solutions. *Chem Eng Sci.* 2004;59:3091–3103.
29. Chanda M, Rempel GL. Chromium(III) removal by poly(ethyleneimine) granular sorbents made by a new process of templated gel filling. *React Funct Polym.* 1997;35:197–207.
30. Chanda M, Rempel GL. Gel-coated ion-exchange resin: a new kinetic model. *Chem Eng Sci.* 1999;54:3723–3733.
31. Li P, Xiu GH, Rodrigues AE. Analytical breakthrough curves for inert core adsorbent with sorption kinetics. *AIChE J.* 2003;49:2974–2979.
32. Li P, Xiu GH, Rodrigues AE. Modeling separation of proteins by inert core adsorbent in a batch adsorber. *Chem Eng Sci.* 2003;58:3361–3371.
33. Li P, Xiu GH, Rodrigues AE. A 3-zone model for protein adsorption kinetics in expanded beds. *Chem Eng Sci.* 2004;59:3837–3847.
34. Rodrigues AE. Permeable packings and perfusion chromatography in protein separation. *J Chromatogr B.* 1997;699:47–61.
35. Lee WC. Protein separation using non-porous sorbents. *J Chromatogr B.* 1997;699:29–45.
36. Kirkland JJ. Superficially porous silica microspheres for the fast high-performance liquid-chromatography of macromolecules. *Anal Chem.* 1992;64:1239–1245.

37. Kirkland JJ, Truszkowski FA, Dilks CH, Engel GS. Superficially porous silica microspheres for fast high-performance liquid chromatography of macromolecules. *J Chromatogr A*. 2000;890:3–13.
38. Satterfield CN. *Heterogeneous Catalysis in Industrial Practice*, 2nd ed. New York: McGraw-Hill, 1991:100.

Appendix

To write the mobile phase equations, Eqs. 18–25, in algebraic form forward difference on time derivative term and backward differences of first- and second-order on special derivative terms are implemented. This leads to

$$\theta_{i,n+1} = \mathrm{AA}_1\theta_{i,n} + \mathrm{AA}_2\theta_{i-1,n} + \mathrm{AA}_3\theta_{i-2,n} - \mathrm{AA}_4(\phi_{i,f-2,n} - 4\phi_{i,f-1,n} + 3\phi_{i,f,n}) \quad \text{(A1)}$$

$$i = 0: \ \theta_{0,n} = 0 \quad \text{(A2)}$$

$$i = ff: \ \theta_{ff-2,n} - 4\theta_{ff-1,n} + 3\theta_{ff,n} = 0 \quad \text{(A3)}$$

$$n = 0: \ \theta_{i,0} = 1 \quad \text{(A4)}$$

where $i = ff$ is the end of the bed at $x = L$, and AA_1, AA_2, AA_3, AA_4 are defined as follows:

$$\mathrm{AA}_1 = 1 - \frac{3\gamma'\Delta(\sigma\tau)}{2\sigma\Delta(\gamma'\zeta)} + \frac{(\gamma')^2\Delta(\sigma\tau)}{\sigma Pe(\Delta(\gamma'\zeta))^2} \quad \text{(A5)}$$

$$\mathrm{AA}_2 = \frac{2\gamma'\Delta(\sigma\tau)}{\sigma\Delta(\gamma'\zeta)} - \frac{2(\gamma')^2\Delta(\sigma\tau)}{\sigma Pe(\Delta(\gamma'\zeta))^2} \quad \text{(A6)}$$

$$\mathrm{AA}_3 = \frac{-\gamma'\Delta(\sigma\tau)}{2\sigma\Delta(\gamma'\zeta)} + \frac{(\gamma')^2\Delta(\sigma\tau)}{\sigma Pe(\Delta(\gamma'\zeta))^2} \quad \text{(A7)}$$

$$\mathrm{AA}_4 = -\frac{\gamma' b}{\sigma(b-a)} \times \frac{\Delta(\sigma\tau)}{2\Delta\rho} \quad \text{(A8)}$$

Equation 3 is obtained using second-order backward difference approximation for the boundary condition $\frac{\partial\theta}{\partial(\gamma'\zeta)}|_{\zeta=1} = 0$.

The descritization of the mobile phase equations, Eqs. 22–25, using central Crank-Nikelson approximations on special terms and forward difference on temporal terms leads to

$$A_j\phi_{i,j+1,n+1} + B_j\phi_{i,j-1,n+1} + F\phi_{i,j,n+1} = -A_j\phi_{i,j+1,n} - B_j\phi_{i,j-1,n} - E\phi_{i,j,n} \quad \text{(A9)}$$

$$j = 0: \ 4\phi_{i,1,n+1} - \phi_{i,2,n+1} - 3\phi_{i,0,n+1} = 0 \quad \text{(A10)}$$

$$j = f: \ \theta_{i,n+1} = \frac{\phi_{i,f,n+1}}{9(1-\phi_{i,f,n+1})} \quad \text{(A11)}$$

$$n = 0: \ \phi_{i,j,0} = 0.9 \quad \text{(A12)}$$

where A_j, B_j, E, and F are defined in Eqs. 47–50.

$$A_j = \frac{\Delta\rho}{j\Delta\rho + a} + 1 \quad \text{(A13)}$$

$$B_j = \frac{-\Delta\rho}{j\Delta\rho + a} + 1 \quad \text{(A14)}$$

$$E = -2 + \frac{4\Delta\rho^2}{\Delta(\sigma\tau)} \quad \text{(A15)}$$

$$F = -2 - \frac{4\Delta\rho^2}{\Delta(\sigma\tau)} \quad \text{(A16)}$$

The discretized model equations, Eqs. A1–A4, and A13–A16, comprise a set of coupled nonlinear Algebraic equations. The C programming language in computational MATLAB media is used to solve this coupled nonlinear system of partial differential equations (PDEs). Because of the inherent nonlinearity of the equations, approximation and error method is used to solve the system of algebraic equations rather than inverse matrix method. Therefore, Eq. A11 may be rephrased as Eqs. A17 and A18.

$$j = f: \ \theta_{i,n+1} = A'\frac{\phi_{i,f,n+1}}{9} \quad \text{(A17)}$$

$$A' = \frac{1}{1-\phi_{i,f,n+1}} \quad \text{(A18)}$$

Now, to solve the system equations, at any node, i, at different times, a single value for $\phi_{i,f,n+1}$ between 0 and 0.9 is guessed, then A' is calculated. By doing this, one will obtain the required matrix of coefficients. Subsequently, the reverse matrix method is implemented and the value of $\phi_{i,f,n+1}$ is obtained. This value is compared with the guessed value. This computation is iterated until the convergence criterion is satisfied. An error of less than 0.0001 was used as convergence criterion. Smaller differences (errors) were attempted, however, that did not lead to appreciable improvement of the results.

Manuscript received Nov. 7, 2008, and revision received Dec. 5, 2008.